

Atomic Structure of a CK2 α Human Kinase by Microfocus Diffraction of Extra-small Microcrystals Grown With Nanobiofilm Template

Eugenia Pechkova^{1,2} and Claudio Nicolini^{2,1*}

¹Fondazione E.L.B.A., Rome, Italy

²Nanoworld Institute and Department of Biophysical M&O Sciences and Technologies, University of Genova, Italy

Abstract Extra-small microcrystals of a human kinase CK2 α were obtained for the first time by the optimization of a recent protein crystallization method based on highly packed protein nanofilm template. Protein crystal induction and growth appear indeed optimal at high surface pressure of the film template yielding high protein orientation and packing. The resulting extra-small CK2 α microcrystals (of about 20 μm in diameter) was subsequently used for synchrotron radiation diffraction data collection, which proves possible by means of the Microfocus Beamline at the ESRF Synchrotron in Grenoble. The quality of the resulting crystal diffraction patterns and of its resulting atomic structure at 2.4 \AA resolution proves the unique validity of the above two combined frontier technologies in defining a new approach to structural proteomics capable to solve the atomic structure of proteins so far never been crystallized and of pharmaceutical relevance. Physical explanation in terms of template dipole moments and possibility of generalization of this method to the wide class of proteins not yet crystallized are finally discussed. The structure of our CK2 α mutant is in the Protein Data Bank (PDB ID Code 1NA7, deposited on 27 November 2002). *J. Cell. Biochem.* 91: 1010–1020, 2004. © 2004 Wiley-Liss, Inc.

Key words: human kinase CK2 α ; lysozyme; crystal growth; synchrotron microfocus; thin film nanotechnology; nanocrystallography

Over the last decade biological macromolecular crystallography has been transformed by the arrival of third generation synchrotron sources. The experimental methodology, however, despite of the recent advances, is not able yet to provide protein crystals over the wide range of proteins of high scientific and industrial interest, remaining the bottleneck of the structural investigation urgently needed for pharmaceutical industry, drug design, and related fields. Indeed, frequently the new methods and the modified classical methods [McPherson and

Shlichta, 1988; Chayen et al., 1992, 2001; Chayen, 1996; Vekilov and Rosenberger, 1998; Tsekova et al., 1999; Fermani et al., 2001; Falini et al., 2002; Adachi et al., 2003] proved in model systems, such as lysozyme can fail in the crystallization of the target proteins [Chayen and Saridakis, 2001]. Despite that every protein needs its own conditions, and in some cases its own methods, to be crystallized; the development of the generalized procedure remains a challenge for crystallographers worldwide.

Among these studies there are many attempts to understand better the physical aspects of crystal nucleation and growth as well as to improve crystal quality [Carter, 1997; Rayment, 1997, 2002; Garcia-Ruiz and Moreno, 1997; Huang et al., 1999; Li et al., 1999; Bunick et al., 2000; Pjura et al., 2000; Nollert et al., 2002; Sauter et al., 2002]; crystallization was also studied in magnetic [Ataka and Wakayama, 2002], electric or ultrasonic fields [Taleb et al., 1999; Nanev and Penkova, 2001], under high pressure [Suzuki et al., 2002] and high temperature [Han and Lin, 2000] centrifugation

Grant sponsor: FIRB-MIUR grant on Organic Nanoscience and Technology (to the University of Genova); Grant sponsor: Italian Ministry of Education, Research and Universities (to the Fondazione E.L.B.A. Coordinates).

*Correspondence to: Prof. Claudio Nicolini, Nanoworld Institute and Biophysics Division-Distbimo, University of Genova 16132 Genova, Italy. E-mail: ando@bf.unige.it

Received 26 February 2003; Accepted 21 June 2003

DOI 10.1002/jcb.10705

© 2004 Wiley-Liss, Inc.

[Pitts, 1992; Lenhoff et al., 1997], levitation [Chung and Trinh, 1998], microgravity [McPherson, 1997; Borgstahl et al., 2001].

Sometimes, advanced techniques which initially appeared to be successful only in individual cases then have been generalized to particular protein type or even entire class of proteins. For example, crystallization in lipidic cubic phase has been used to obtain good quality three-dimensional (3D) microcrystals crystals of bacteriorhodopsin (bR), analyzed by synchrotron microfocus [Landau and Rosenbusch, 1996]. This study gives a new route to membrane protein crystallization.

In the present work, we discuss the optimization of recently introduced nanotechnology based protein crystallization method, initially proven with the crystallization of lysozyme [Pechkova and Nicolini, 2001] and cytochrome P450scc [Pechkova and Nicolini, 2002a,b], for the production of diffracting crystal of the human protein kinase CK2 α , protein with high oncogenic potential.

While the crystal structure of the recombinant catalytic subunit of CK2 from *Zea mays* has been determined [Niefind et al., 1999], the human CK2 α subunit until now resisted the crystallization attempts by traditional vapor diffusion methods, the reason of it being probably its pronounced overall instability.

Only with the implementation of nanostructured thin protein film template, the long lasted failure on human CK2 α crystallization was overcome [Pechkova and Nicolini, 2002b], but diffraction data could not be obtained by common X-ray diffractometer methods and by the second generation Electra Synchrotron in Trieste likely due the very small dimension of the obtained microcrystals [Pechkova and Nicolini, 2002b].

While earlier findings have shown the positive effect of thin protein film template on the crystal growth of different class of proteins [Pechkova and Nicolini, 2001, 2002a,b], open questions still remain on the possibilities to further optimize the method improving both the extent of protein's crystal nucleation and growth with increasing surface pressure of protein film template and the diffraction properties of the crystals grown by thin film nanotechnology [Pechkova and Nicolini, 2002a]. Both questions are answered here utilizing a protein model as the egg white lysozyme. Physical explanation in terms of template dipole

moments is discussed with generalization of this method to the wide class of proteins not yet crystallized as human CK2 α kinase.

Opportunities posed by the third generation Synchrotron in Grenoble allow to analyze these microcrystals previously unusable [Cusack et al., 1998] and in our case, to collect the entire diffraction data set from a single microcrystal with the use of microfocus synchrotron radiation. The quality of the resulting crystal diffraction patterns prove the unique validity of the above two combined frontier technologies (see Fig. 1) in defining a new approach to structural proteomics capable to solve the atomic structure of proteins so far never been crystallized and of pharmaceutical relevance.

The structure of human CK2 α kinase, here summarized as originally deposited in the Protein Data Bank on November 27, 2002 (PDB ID Code 1NA7) and given in full crystallographic details in Pechkova et al. [2003], constitute a significant proof of principle of this nanotechnology-based approach.

EXPERIMENTAL PROCEDURES

Protein Preparation

Chicken egg white lysozyme was purchased from Sigma (Milan, Italy); the stock solution was prepared as previously described Pechkova and Nicolini [2001].

A three single-point mutant (Lys10Ser, Glu27Ala, Lys76Asn) of the catalytic subunit of human CK2 α was expressed in *Escherichia coli* and purified according to a previously described method [Battistutta et al., 2001]. Human recombinant CK2 α was concentrated by centrifugation with Centricon Centrifugal Membrane filter (Cut-off 10,000 Da MW). The final protein concentration was about 8 mg/ml in 25 mM NaCl, 0.05% NaN₃, 7 mM β -mercaptoethanol, 25 mM Tris-HCl buffer, pH 8.5. Protein purity after purification and concentration was controlled by SDS-PAGE as shown in [Pechkova et al., 2003]. To monitor the effect of protein degradation, the sample was maintained at 20°C during few days. Degradation bands appeared only after 3 days as shown in Nicolini 2002b and Pechkova et al. [2003].

Optimization of the Nanotechnology-Based Template Method

Langmuir-Blodgett (LB) technique and namely its variation, a modified Langmuir-

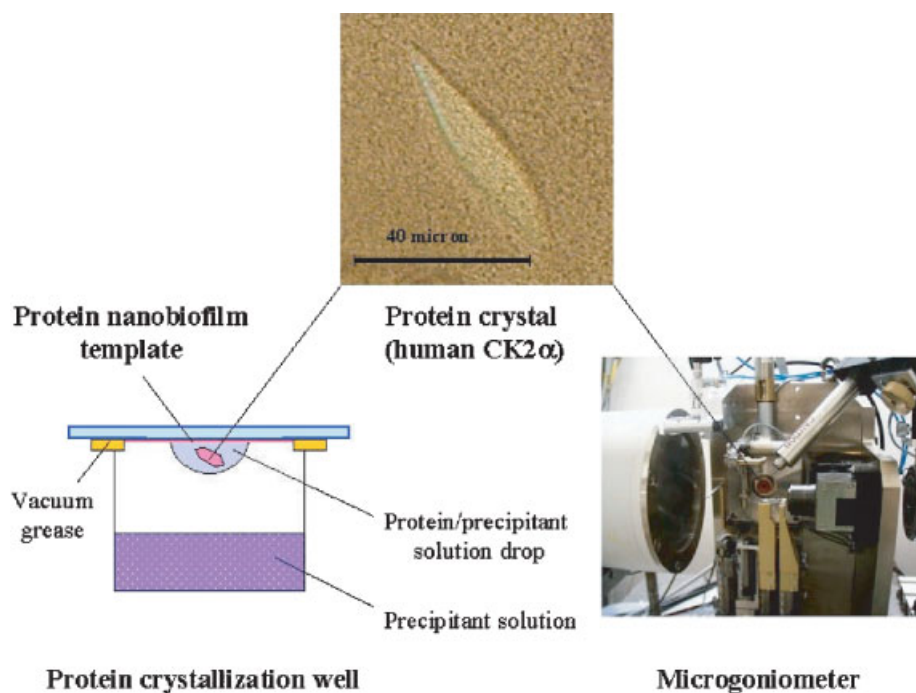


Fig. 1. Nanotechnology based crystallization method utilizing a modified hanging drop vapor diffusion and an homologous protein template produced by Langmuir–Blodgett (LB) trough. Microgoniometer at Synchrotron Microfocus is also shown (courtesy of C. Rieker).

Schaeffer (LS) method used in different fields of science and technology [Nicolini, 1996a,b, 1997], is utilized here. The proteins were brought to air–water interface and then compressed to the desired surface pressure by means of LB trough [Nicolini, 1997] with distilled water or appropriate buffer solution used as a subphase. The proteins monolayers were compressed immediately after spreading with a compression speed of 10–100 cm/min, depending of the trough size and the nature of the protein. The more soluble the protein is, the faster the through barriers should be moved. Surface pressure area isotherms measurements were performed to characterize the protein monolayer at the air–water interface compressed in a wide range of milliNewton per meter. Different parameters were been varying with the goal to reach the optimal isotherm: protein concentration, compression velocity, subphase composition. The transfer of protein monolayer from the subphase (water or buffer) surface onto solid support was performed by touching the support in parallel to the subphase surface according to LS technique (horizontal lift) [Nicolini, 1997] at the desired protein surface pressure. Siliconized circle glass cover slide (Hampton Research, Laguna Niguel, CA)

washed in distilled water and drayed in nitrogen flux were used as substrate for the protein thin film deposition. As it shown in Figure 1 protein monolayer transferred from the air–water interface onto the siliconized glass cover slide was used as a template for modification of classical vapor diffusion hanging drop method [Pechkova and Nicolini, 2002a,b]. During the crystallization procedure the following parameters were varied: precipitant nature and concentration, protein monolayer surface pressure during template preparation, number of the protein monolayers in protein nanobiofilm template. All experiments were carried out at the controlled temperature of 20°C.

Crystallization Procedures

Classical hanging drop method was successfully used for lysozyme crystal formation at the following optimized conditions: 20 mg/ml lysozyme acetate buffer solution (pH 4.5) and 0.3 M NaCl in hanging drop equilibrated against 1,000 ml reservoir of 0.6 M NaCl solution. For comparison, the same condition was utilized for lysozyme crystallization by thin film template method. In this series of experiments the protein monolayer pressure was varied in a wide range as shown later in the “Results.”

In case of human protein kinase CK2 α , successful crystallization trials were made by mixing a 2 μ l drop of above stock solution with 2 μ l of precipitant solution (25% PEG 3500, sodium acetate 0.2 M, Tris 0.1 M pH 8). This 4 μ l drop was plated onto thin CK2 α film, deposited on the siliconized glass slide at protein monolayer pressure 20 mN/M. The drop was equilibrated against 700 ml reservoir of the same precipitant solution (25% PEG 3500). Crystals grew in few days at 293°K.

Synchrotron Radiation Microfocus Diffraction

Focused X-ray beam from third generation synchrotron sources are used for the characterization of our ultra-small protein crystals.

For the experiments here reported, Microfocus beam-line ID-13 at the ESRF (beam size 20 \times 20 μ m²) has been used. This beam width is capable to obtain X-rays diffraction patterns from microcrystals of less than 50 μ m micron, possibly down to 5 μ m [Cusack et al., 1998]. The main instrumental setup being used by us during our experimentation has been the microgoniometer developed for protein crystallography with typical beam sizes of 5–10 μ m based on a condensing mirror and collimators (see Fig. 1). The wavelength used was 0.955 Å and the crystal-to-detector distance 120 mm. Diffraction data were collected at a temperature of 100°K. Crystals were fished from the mother liquid and frozen in a nitrogen stream, without using any cryo-protectant solution.

Lysozyme crystals prepared by classical hanging drop method and by nanotechnology-based method were mounded in cryoloops of appropriate diameter (1 mm) and used for data collection in order to compare their diffraction quality.

Two needle CK2 α crystals of approximate size 60 \times 20 \times 20 μ m³ and 110 \times 20 \times 20 μ m³ were analyzed. Crystals diffract to a maximum resolution of 2.4 Å. The one single crystal 60 \times 20 \times 20 μ m³ used to collect a complete data set for further CK2 α 3D atomic structure determination.

Diffraction data were collected at a temperature of 100°K. Crystals were fished from the mother liquid and frozen in a nitrogen stream, without using any cryo-protectant solution.

As shown in Pechkova et al. [2003], CK2 α crystals belong to space group P2₁, with $a = 58.68$ Å, $b = 45.95$ Å, $c = 63.96$ Å, and $\beta = 111.8$ Å. One molecule is present in the asym-

metric unit. It is worth to notice that the space group and cell parameters of human CK2 α crystals differ from those of the *Zea mays* protein. Assuming a molecular mass of approximately 40,000, the V_M coefficient is 2.0 Å³ Da⁻¹, whilst if the molecular mass of the protein is 45,000 V_M it becomes 1.78 Å³ Da⁻¹ [Pechkova et al., 2003].

Data were indexed and integrated with MOSFLM [Leslie, 1991], and then scaled with the program SCALA from the CCP4 software package [CCP4, 1994]. The crystal structure was solved by the molecular replacement method with the program AMORE [Navaza, 1994], using the structure of the CK2 α subunit from *Zea mays* as a template (PDB ID code 1JAM). The crystallographic refinement of the structure was carried out with the CNS software package [Brunger et al., 1998] alternated with manual inspection of the electron density maps and rebuilding of the model using the graphic program QUANTA, 1986.

The full statistics on data collection, processing and refinement are given in details in Pechkova et al. [2003]. The final model presents an overall R factor of 0.209 (R_{free} 0.273) with 91 water molecules and a good stereochemistry.

RESULTS

In order to understand better the physical aspects of protein thin film template influence on crystal growth as well as to improve crystal size and quality, different templates were tested in the nanotechnology based crystallization method (see Fig. 1). The protein crystal size was evaluated as function of surface pressure of protein monolayer during thin film deposition, utilizing lysozyme as the model system. Lysozyme thin film template prepared at the different protein surface pressure was utilized in crystallization by nanofilm template method.

Generally, the protein dimensions, solubility, and surface charge distribution influence on surface pressure value. It should be born in mind that the surface pressure can be also influenced by subphase composition. Systematic search on the effect of it is carried out to optimize further crystal nucleation and growth.

Figure 2 shows the lysozyme crystals growth versus time up to 50 h, for homologous thin film template prepared with increasing surface pressures at the air–water interface (respectively at 10, 15, 20, 25, and 30 mN/m). The

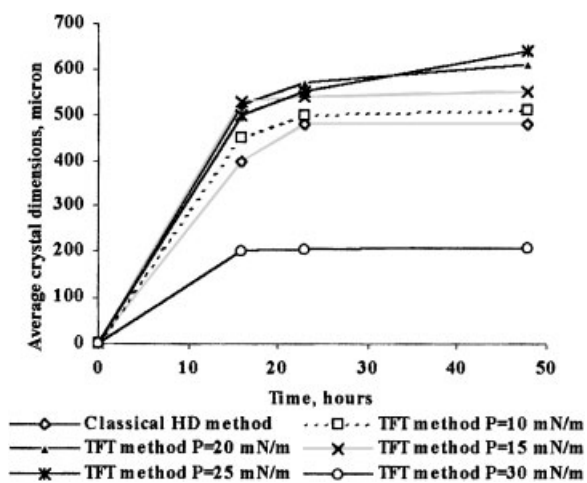


Fig. 2. Lysozyme crystals size by modified classical and hanging drop method versus time for different surface pressure at the air–water interface of the homologous thin LB film template. The ionic strength was 0.6 M and the protein concentration was 20 mg/ml in the crystallization drop.

optimized crystallization condition at which the largest lysozyme protein have been obtained by classical hanging drop method have been chosen for thin film template method in order to evidence templates influence on protein crystal growth. Optimal surface pressure is 25 mN/m corresponding to the most closely packed and oriented lysozyme monolayer, before it collapses at 30 mN/m as apparent by Brewster microscopy (data not shown) with a pronounced decreased of crystal growth (Fig. 2). The optimal mean size of the obtained lysozyme crystals after a week of equilibration was 800 μm while crystals obtained in equal conditions but with the classical method were only 600 μm [Pechkova and Nicolini, 2001]. Such a large lysozyme crystals was easily mounted in 1,000 μm nylon loop for diffraction data collection (see later Fig. 5d).

The diffraction quality of lysozyme crystals grown by classical and modified hanging drop method was compared. Figure 3 shows the lysozyme crystals obtained with (b, right) and without (a, left) thin film template and their corresponding synchrotron diffraction patterns obtained at 1.7 Å the Microfocus Beamline. As it is apparent from the Figure 3, the first diffraction pattern is clearly better than the second one.

In the case of human CK2 α kinase, the LS nanofilm template are prepared at 20 mN/m surface pressure to warrant high template packing, confirmed by nanogravimetry [Pechkova

and Nicolini, 2002b]. Under this optimized crystallization condition, needle human CK2 α microcrystals different sizes were grown to different sizes as shown in Figure 4. In Figure 5 human CK2 α microcrystal of $110 \times 20 \times 20 \mu\text{m}^3$ (b) are shown mounted on the nylon loop for their subsequent exposure to the Microfocus Synchrotron Beamline.

Figure 6 shows the effect of 4 h exposure to the Microfocus Synchrotron Beamline on a human CK2 α microcrystal of $60 \times 20 \times 20 \mu\text{m}^3$ during the collection of data diffraction utilized for the subsequent 3D atomic structure determination [Pechkova and Nicolini, 2003b]. The Synchrotron diffraction pattern of the human CK2 α microcrystal is shown in Figure 7. The diffraction data could be obtained for the first time at 2.4 Å resolution on this very small human CK2 α microcrystal (Fig. 6) obtained by the optimized homologous protein thin film template. Due to the very small size of the crystals (of about 20 μm in diameter), diffraction data could be collected only using the microfocus beamline of $20 \times 20 \mu\text{m}^2$ at the ID13 beamline of ESRF (Grenoble), which has utilized with great success in many other experimental circumstances [Pebay-Peyroula et al., 1997; Riek et al., 1997; Cusack et al., 1998; Muller et al., 1998; Ekström et al., 2003].

One human kinase CK2 α needle crystal of approximate size $60 \times 20 \times 20 \mu\text{m}^3$ was enough for collecting a complete data set and the subsequent 3D atomic structure determination at 2.4 Å resolution [Pechkova et al., 2003].

The maximum resolution obtained, 2.4 Å, is quite good, considering the very small size of the crystal used. A portion of the electron density around residues from 197 to 200, 216 to 220, and 305 to 307 (Fig. 8) shows the quality of the map, which is generally quite well defined. Residues from 5 to 329 could be located in the map, whilst a short part of the N-terminus (residues from 1 to 4) and the entire C-terminal end (61 residues from 330 to 390) were not visible.

The presence of the significant space in the crystal cell in correspondence of the C-terminus [Pechkova et al., 2003; PDB code 1NA7] seems to confirm the existence of a tail formed of these residues, highly disordered, and thereby not visible. Another possibility is that human CK2 α has undergone proteolytic degradation at the C-terminal end during purification and/or crystallization, but this is not compatible with the existence of a very small degradation band

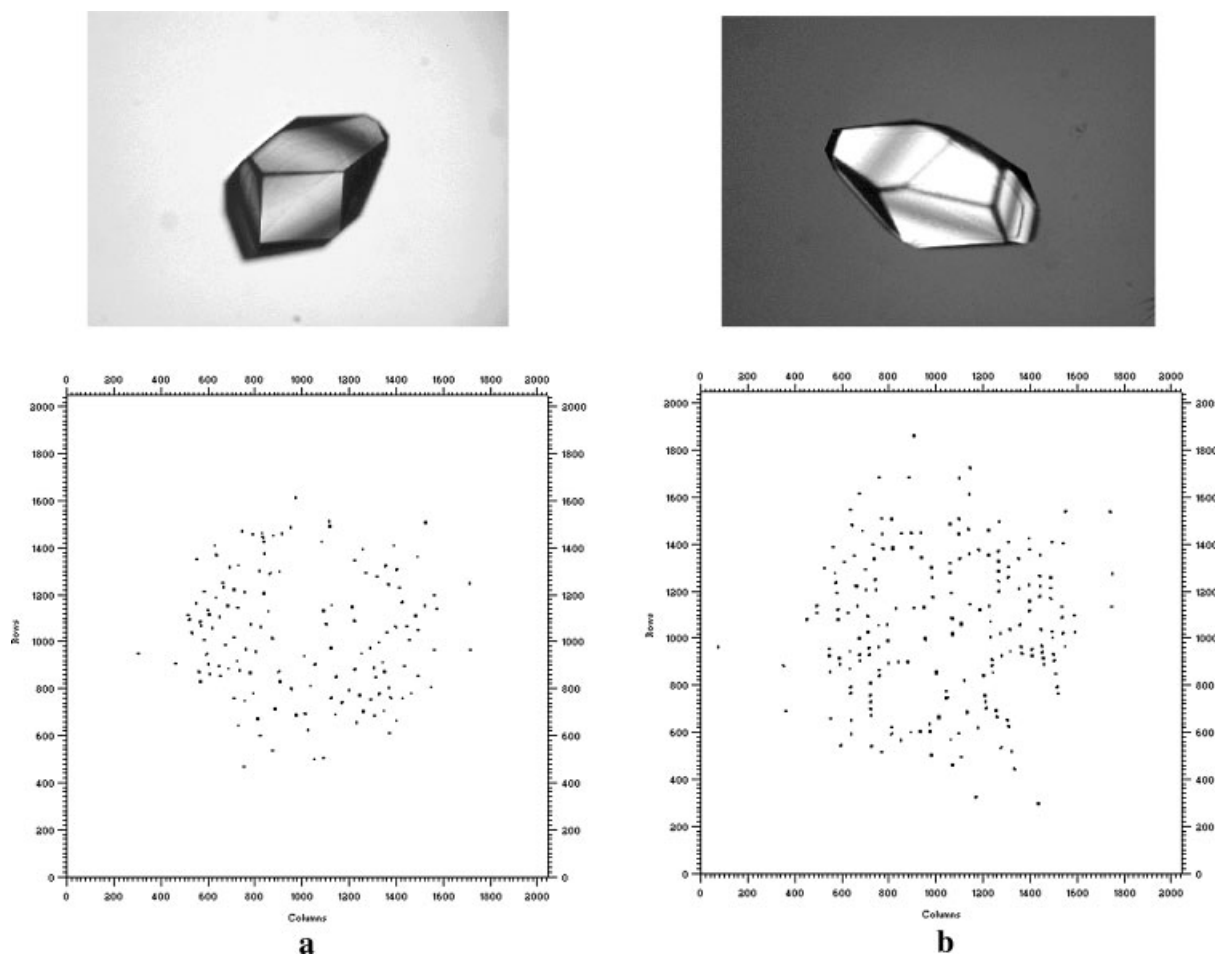


Fig. 3. Lysozyme crystals obtained by classical hanging drop method (a), 600 μm along the longest axis and by nanobiofilm template method (b), 800 μm along the longest axis. Their corresponding synchrotron diffraction pattern are presented below.

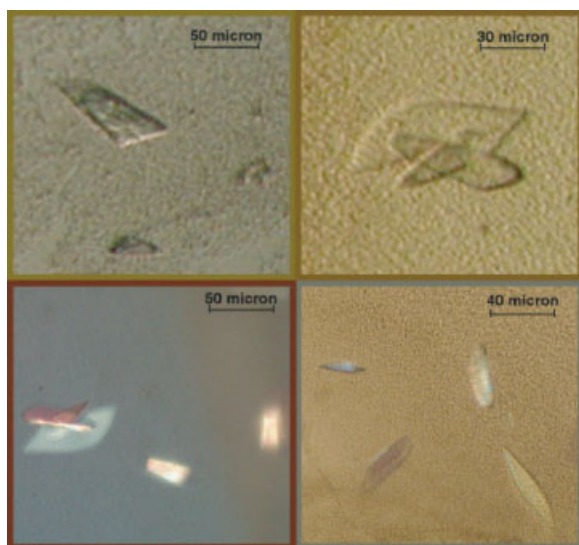


Fig. 4. Human CK2 α microcrystals obtained by the protein nanofilm template.

which does not change during purification steps and in the entire time of crystal formation. From our gel electrophoresis results it would appear very unlikely that the protein crystallized is a truncated catalytic subunit. Indeed, it was our experience [Pechkova and Nicolini, 2002b] that in both forms of CK2 α , truncated and untruncated, the same results were obtained with our thin film nanotechnology in terms of microcrystal nucleation and growth. The latter point is supported by the fraction of the solvent content of the crystal, which has the still acceptable value of about 31% of the total crystal volume if the entire molecule is assumed present in the asymmetric unit, whilst it increases to about 39% if we consider a truncated protein.

In summary, both possibilities strongly suggest that the long C-terminal tail is flexible, at least in the isolated catalytic subunit.

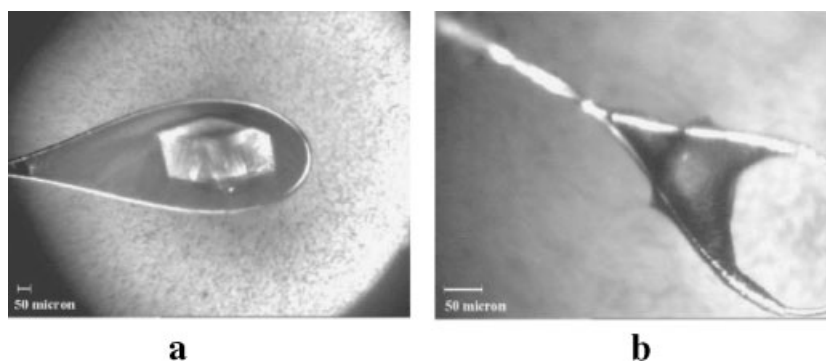


Fig. 5. **a:** Large lysozyme crystal and **(b)** human CK2 α microcrystal mounted on the nylon loop and exposed to the Microfocus Synchrotron Beamline for the collection of diffraction data utilized for the subsequent 3D atomic structure determination.

The overall structure of the human CK2 α presents the classic fold of the catalytic subunit of protein kinases, formed by two domains: a N-terminal domain, mainly composed by β -strands, and a C-terminal domain, containing several α -helices (Fig. 9). Ramachandran plot of the conformational angles Φ and Ψ at each α -carbon atom of the kinase main chain is shown in Figure 10. For further details see Pechkova et al. [2003]. The structure CK2 α was deposited in the Protein Data Bank on 27 November 2002 (PDB ID Code 1NA7) and presented preliminarily at the International Symposium on Diffraction Structural Biology on 28 May 2003 in Tsukuba (Japan). It was also discussed in the Ph.D. thesis of Eugenia Pechkova “Protein crystallography by thin film nanotechnology,” defended on 20 March, 2003 at the University of Genova, Italy.

DISCUSSION

Several conclusions can be drawn from the data here presented about the optimization of

our method based on the protein template obtained by thin film nanotechnology and on the modification of the classical vapor diffusion hanging drop method [Pechkova and Nicolini, 2001, 2002a,b]:

- enhancement of crystal nucleation and growth;
- optimal resolution of the X-rays diffraction patterns.

Protein’s crystal growth in presence of thin protein film template is shown to be critically dependent on the orientation of proteins in the thin film until reaching a reproducible plateau value. The orientation appears properly controlled by changing the surface pressure at the air–water interface where the protein films are formed [Troitsky et al., 1996; Nicolini, 1997].

By exploring crystal size dependency on the homologous template surface pressure, the optimal protein surface pressure to be chosen for the deposition appears to correspond to the most highly packed ordered monolayer. This

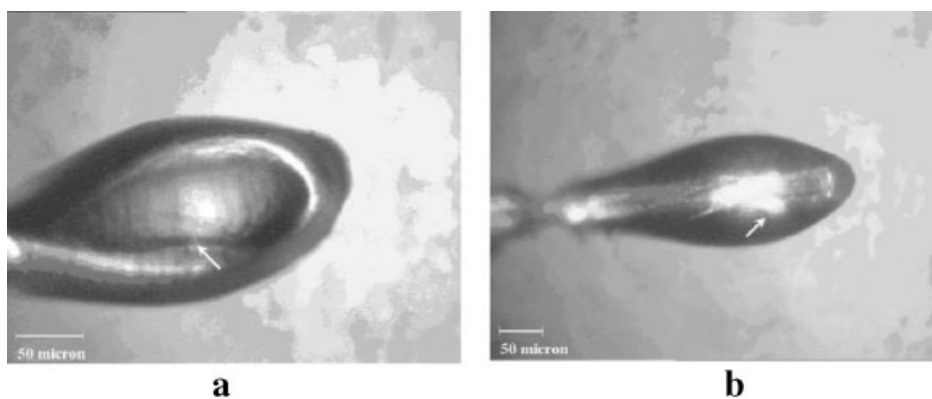


Fig. 6. Human CK2 α microcrystal mounted on the nylon loop before **(a)** and after **(b)** exposure to the Microfocus Synchrotron Beamline for the collection of complete diffraction data set.

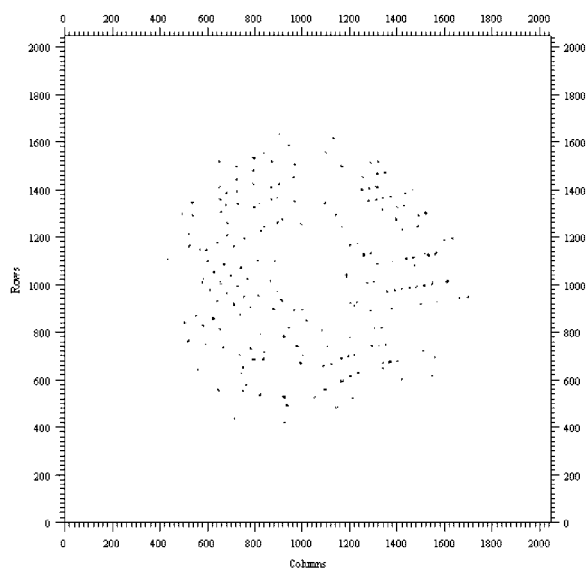


Fig. 7. Synchrotron diffraction pattern of human CK2 α microcrystal.

optimized procedure extended to the mutant of the human catalytic subunit CK2 α proves successful in obtaining diffraction quality microcrystals. Using third generation synchrotron, namely at the microfocus beamline of $20 \times 20 \mu\text{m}^2$ at ESRF in Grenoble [Cusack et al., 1998; Perrakis et al., 1999], it became possible to resolve human protein kinase CK2 α catalytic subunit at rather high resolution.

Furthermore, the small CK2 α microcrystals of only a few micron in size, before unusable for the structural analysis, appear quite stable to the incoming considerable radiation. Indeed, despite of longtime exposure microcrystals appear to preserve their shape and size without any apparent damage. Stability and high diffraction quality of human CK2 α single microcrystal of $60 \times 20 \times 20 \mu\text{m}^3$ allowed to collect a

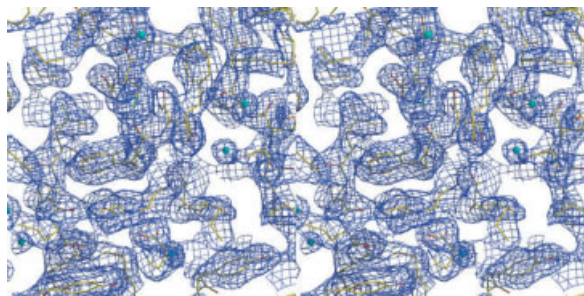


Fig. 8. Representation of the portion of the human CK2 α electron density map (residues from 197 to 200, 216 to 220, and 305 to 307), obtained with coefficients $|2F_{\text{obs}} - F_{\text{calc}}|$ and calculated phases. Contours are drawn at $1\sigma(I)$ level. For further details see Pechkova et al. [2003].

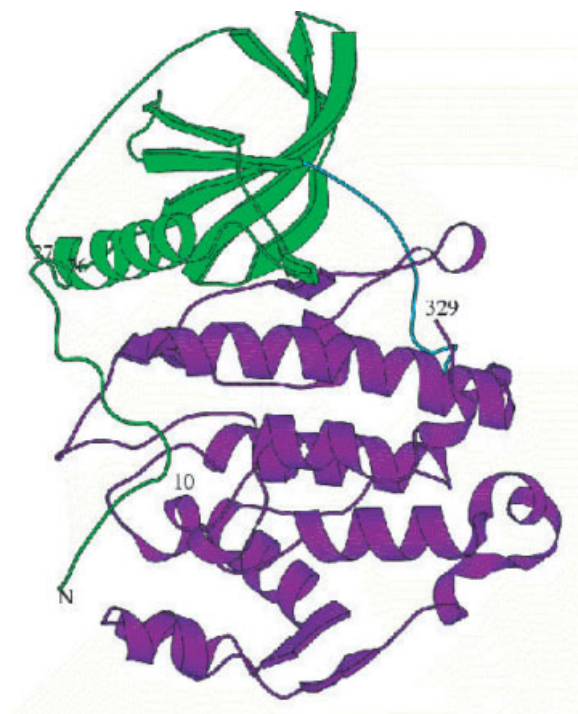
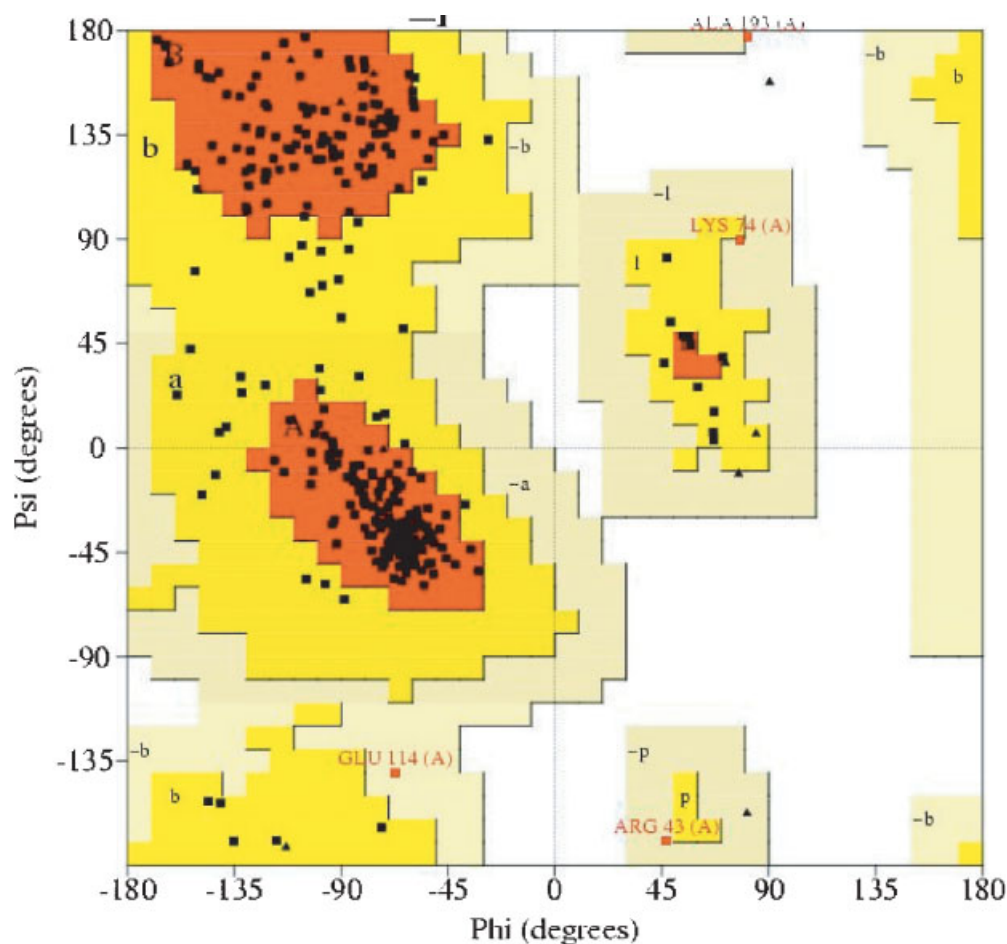


Fig. 9. Cartoon representation of the three-dimensional (3D) atomic structure of human CK2 α . The N-terminal domain is in green, the C-terminal one in magenta. For further details see Pechkova et al. [2003].

complete 2.4 Å data set at Microfocus Synchrotron Beamline (Fig. 6). The similar result at Microfocus ESRF was obtained with single bR crystal of about $30 \times 30 \times 5 \mu\text{m}^3$, producing an entire 2.4 Å data set, which led to the first high resolution model of bR obtained by X-ray crystallography [Pebay-Peyroula et al., 1997].

Finally, it should not escape our notice that a possible physical explanation of the increased crystal growth with our method [Pechkova and Nicolini, 2001, 2002a,b, 2003a,b] emerges from the variation in template surface pressure (Fig. 2). The increased anisotropy in thin film template associated to the increased surface pressure [Nicolini, 1996a] is causing a protein orientation and thereby a dipole moment in the LB monolayer. Indeed, in previous studies [Dubrovsky and Nicolini, 1994; Facci et al., 1994; Nicolini et al., 2001], surface potential varies from -0.2 mV in the self-assembly (randomly oriented proteins) to -80 mV in the LB film (ordered and oriented proteins). This dipole moment could be the cause of the controllable and predictable nucleation and growth of the protein crystals never so far obtained, namely of the entire catalytic subunit



Plot statistics:

Residues in most favoured regions (a, b, l)	247	82.9%
Residues in additional allowed regions (a, b, l, p)	47	15.8%
Residues in generously allowed regions (-a, -b, -l, -p)	3	1.0%
Residues in generously allowed regions	1	0.3%
Total number of residues	326	

Fig. 10. Ramachandran plot of the conformational angles Φ and Ψ at each α -carbon atom of the human CK2 kinase main chain. For further details see Pechkova et al. [2003].

of human CK2 kinase here shown and of the cytochrome P450 scc [Pechkova and Nicolini, 2003a,b].

In all proteins systems being so far studied indeed the surface potential in the thin protein films increases significantly pointing to the increased anisotropy which in turn could trigger the nucleation and crystal growth, including those proteins so far not crystallizable.

ACKNOWLEDGMENTS

We thank Giuseppe Zanotti for his valuable advice in crystal preparation and structure refinement; and to the beamline staff of ID13 at ESRF/EMBL, Grenoble, Christian Riek, Manfred Burghammer and David Flot for excellent conditions and support during data collection. Coordinates have been deposited in

the Protein Data Bank with accession code 1NA7 (27 November 2002).

REFERENCES

- Adachi H, Takano K, Morikawa M, Kanaya S, Yoshimura M, Mori Y, Sasaki T. 2003. Application of a two-liquid system to sitting-drop vapour-diffusion protein crystallization. *Acta Crystallogr D Biol Crystallogr* 59:194–196.
- Ataka M, Wakayama NI. 2002. Effects of a magnetic field and magnetization force on protein crystal growth. Why does a magnet improve the quality of some crystals? *Acta Crystallogr D Biol Crystallogr* 58:1708–1710.
- Battistutta R, De McLingre, Sarno S, Zanotti G, Pinna LA. 2001. Structural features underlying selective inhibition of protein kinase CK2 by ATP site-directed tetrabromo-2-benzotriazone. *Protein Science* 10:2200–2206.
- Borgstahl GE, Vahedi-Faridi A, Lovelace J, Bellamy HD, Snell EH. 2001. A test of macromolecular crystallization in microgravity: Large well ordered insulin crystals. *Acta Crystallogr D Biol Crystallogr* 57:1204–1207.
- Brunger AT, Adams PD, Clore GM, DeLano WL, Gros P, Grosse Kunstleve RW, Jiang JS, Kuszewski J, Nilges M, Pannu NS, Read RJ, Rice LM, Simonson T, Warren GL. 1998. Crystallography & NMR system: A new software suite for macromolecular structure determination. *Acta Crystallogr D* 54:905–921.
- Bunick C, North AC, Stubbs G. 2000. Evaporative microdialysis: An effective improvement in an established method of protein crystallization. *Acta Crystallogr D Biol Crystallogr* 11:1430–1431.
- Carter CW. 1997. Response surface methods for optimizing and improving reproducibility of crystal growth. *Methods Enzymol* 276:74–99.
- CCP4. 1994. Collaborative computational project number 4. *Acta Crystallogr D* 50:760–763.
- Chayen NE. 1996. A novel technique for containerless protein crystallization. *Protein Eng* 9:927–929.
- Chayen NE, Saridakis E. 2001. Is lysozyme really the ideal model protein? *J Cryst Growth* 232:262–264.
- Chayen NE, Patrick D, Shaw S, Blow DM. 1992. Microbatch crystallization under oil—A new technique allowing many small-volume crystallization trials. *J Cryst Growth* 122:176–180.
- Chayen NE, Saridakis E, El-Bahar R, Nemirovsky Y. 2001. Porous silicon: An effective nucleation-inducing material for protein crystallization. *J Mol Biol* 312:591–595.
- Chung SK, Trinh EH. 1998. Containerless protein crystal growth in rotating levitated drops. *J Cryst Growth* 194:384–397.
- Cusack S, Bernali H, Bram A, Burghammer M, Perrakis A, Riekel C. 1998. Small is beautiful: Protein micro-crystallography. *Nat Struct Biol* 5:634–637.
- Dubrovsky T, Nicolini C. 1994. Preparation and immobilization of Langmuir–Blodgett films of antibodies conjugated to enzyme for potentiometric sensor application. *Sensors Actuators* 22:69–73.
- Ekström F, Stier G, Sauer UH. 2003. Crystallization of the actin-binding domain of human-actinin: Analysis of microcrystals of SeMet-labelled protein. *Acta Cryst D* 59:724–726.
- Facci P, Erokhin V, Nicolini C. 1994. Scanning tunneling microscopy of a monolayer of reaction centers. *Thin Solid Films* 243:403–406.
- Falini G, Fermani S, Conforti G, Ripamonti A. 2002. Protein crystallisation on chemically modified mica surfaces. *Acta Crystallogr D Biol Crystallogr* 58:1649–1652.
- Fermani S, Falini G, Minnucci M, Ripamonti A. 2001. Protein crystallization on polymeric film surfaces. *J Cryst Growth* 224:327–334.
- Garcia-Ruiz JM, Moreno A. 1997. Growth kinetics of protein single crystals in the gel acupuncture technique. *J Cryst Growth* 178:393–401.
- Han Q, Lin S-X. 2000. The study of crystallization of estrogenic 17 β -hydroxysteroid dehydrogenase with DHEA and DHT at elevated temperature. *Biochem Biophys Res Commun* 277:100–106.
- Huang QQ, Teng MK, Niu LW. 1999. Protein crystallization with a combination of hard and soft precipitants. *Acta Crystallogr D Biol Crystallogr* 55:1444–1448.
- Landau EM, Rosenbusch JP. 1996. Lipidic cubic phases: A novel concept for the crystallisation of membrane proteins. *Proc Natl Acad Sci USA* 93:14532–14535.
- Lenhoff AM, Pjura PE, Dilmore JG, Godlewski TS, Jr. 1997. Ultracentrifugal crystallization of proteins: Transport-kinetic modelling, and experimental behavior of catalase. *J Cryst Growth* 180:113–126.
- Leslie AGW. 1991. Moras VD, Podjarny AD, Thierry JP, editors. *Crystallographic computing*. Oxford: Oxford University Press. pp 27–38.
- Li H, Nadarajah A, Pusey ML. 1999. Molecular replacement in P450 crystal structure determinations. *Acta Crystallogr D Biol Crystallogr* 55:1036–10345.
- McPherson A. 1997. Recent advances in the microgravity crystallization of biological macromolecules. *Trends Biotechnol* 15:197–200.
- McPherson A, Shlichta P. 1988. Heterogeneous and epitaxial nucleation of protein crystals on mineral surfaces. *Science* 239:385–387.
- Muller M, Czihak C, Vogl G, Fratzl P, Schober H, Riekel C. 1998. Direct observation of micro arrangement in a single native cellulose fiber by X-ray small-angle scattering. *Macromolecules* 31:3953–3957.
- Nanev C, Penkova A. 2001. Nucleation of lysozyme crystals under external electric and ultrasonic fields. *J Cryst Growth* 232:285–293.
- Navaza J. 1994. AMORE—An automated package for molecular replacement. *Acta Crystallogr A* 50:157–163.
- Nicolini C. 1996a. *Molecular Bioelectronics*. New York: World Scientific. pp 1–266.
- Nicolini C. 1996b. Supramolecular architecture and molecular bioelectronics. *Thin Solid Film* 284:285:1–5.
- Nicolini C. 1997. Protein monolayer engineering: Principles and application to biocatalysis. *Trends Biotechnol* 15: 395–401.
- Nicolini C, Erokhin V, Ghisellini P, Paternolli C, Ram MK, Sivozhelezov V. 2001. P450scc engineering and nanostructuring for cholesterol sensing. *Langmuir* 17:3719–3726.
- Niefind K, Putter M, Guerra B, Issinger OG, Schomburg D. 1999. CTP plus water mimic ATP in the active site of protein kinase CK2. *Nat Struct Biol* 6:1100–1103.
- Nollert P, Navarro J, Landau EM. 2002. Crystallization of membrane proteins in cubo. *Methods Enzymol* 343: 183–199.
- Pebay-Peyroula E, Rummel G, Rosenbusch JP, Landau EM. 1997. X-ray structure of bacteriorhodopsin at 2.5 Angstroms from microcrystals grown in lipidic cubic phases. *Science* 227:1676–1681.

- Pechkova E, Nicolini C. 2001. Accelerated protein crystal growth onto the protein thin film. *J Cryst Growth* 231: 599–602.
- Pechkova E, Nicolini C. 2002a. From art to science in protein crystallization by means of thin film nanotechnology. *Nanotechnology* 13:460–464.
- Pechkova E, Nicolini C. 2002b. Protein nucleation and crystallization by homologous protein thin film template. *J Cell Biochem* 85:243–251.
- Pechkova E, Nicolini C. 2003a. Protein nanocrystallography: A new approach to structural proteomics (Opinion article). *Trends Biotechnol* (in press).
- Pechkova E, Nicolini C. 2003b. Proteomics and nanocrystallography. New York: Kluwer-Plenum. pp 1–210.
- Pechkova E, Zanotti G, Nicolini C. 2003. Three-dimensional atomic structure of the mutant of the catalytic subunit of human kinase ck2. *Acta Cryst D59*: (in press).
- Perrakis A, Cipriani F, Castagna JC, Claustre L, Burghammer M, Riekkel C, Cusack S. 1999. Protein microcrystals and the design of a microdiffractometer: Current experience and plans at EMBL and ESRF/ID13. *Acta Crystallogr D Biol Crystallogr* 55:1765–1770.
- Pitts JE. 1992. Crystallization by centrifugation. *Nature* 355:117.
- Pjura PE, Lenhoff AM, Leonard SA, Gittis AG. 2000. Protein crystallization by design: Chymotrypsinogen without precipitants. *J Mol Biol* 300:235–239.
- QUANTA. 1986. Version 98. 1111, Molecular Simulation, Inc. 191.
- Rayment I. 1997. Reductive alkylation of lysine residues to alter crystallization properties of proteins. *Methods Enzymol* 276:171.
- Rayment I. 2002. Small-scale batch crystallization of proteins revisited: An underutilized way to grow large protein crystals. *Structure* 10:147–151.
- Riekkel C, Cedola A, Heidelbach F, Wagner K. 1997. Microdiffraction experiments on single polymeric fibres by synchrotron radiation. *Macromolecules* 30:1033–1037.
- Sauter C, Lorber B, Giege R. 2002. Towards atomic resolution with crystals grown in gel: The case of thaumatin seen at room temperature. *Proteins* 48:146–150.
- Suzuki Y, Sazaki G, Miyashita S, Sawada T, Tamura K, Komatsu H. 2002. Protein crystallization under high pressure. *Biochim Biophys Acta* 1595:345–356.
- Taleb M, Didierjean C, Jelsch C, Mangeot JP, Capelle B, Aubry A. 1999. Crystallization of proteins under an external electric field. *J Cryst Growth* 200:575–582.
- Troitsky VI, Sartore M, Berzina S, Nardelli D, Nicolini C. 1996. Instrument for depositing Langmuir–Blodgett films of alternatine monolayers using a protective layer. *Rev Sci Instrum* 67:4216–4223.
- Tsekova D, Dimitrova S, Nanev C. 1999. Heterogeneous nucleation (and adhesion) of lysozyme crystals. *J Cryst Growth* 196:226–233.
- Vekilov PG, Rosenberger F. 1998. Protein crystal growth under forced solution flow: Experimental setup and general response of lysozyme. *J Cryst Growth* 186:251–261.